

PAPER

A study of electroactive polyvinyl chloride (PVC) gel actuators through the use of the electric modulus formalism and cyclic linear voltage sweeps

To cite this article: Zachary Frank *et al* 2022 *Smart Mater. Struct.* **31** 035020

View the [article online](#) for updates and enhancements.

You may also like

- [Dynamic braille display based on surface-structured PVC gel](#)
Chengbo Tian, Min Yu, Yuwei Wu et al.
- [A study of mechanoelectrical transduction behavior in polyvinyl chloride \(PVC\) gel as smart sensors](#)
Justin Neubauer, Zakai J Olsen, Zachary Frank et al.
- [Deformable polyvinyl chloride gel for fabrication of varifocal microlens array](#)
Yasumi Yamada, Hideyuki Emori and Toshihiro Hirai



ECS
The
Electrochemical
Society
Advancing solid state &
electrochemical science & technology

DISCOVER
how sustainability
intersects with
electrochemistry & solid
state science research

A study of electroactive polyvinyl chloride (PVC) gel actuators through the use of the electric modulus formalism and cyclic linear voltage sweeps

Zachary Frank¹ , Mohammed Al-Rubaiai² , Xiaobo Tan² and Kwang J Kim^{1,*} 

¹ Active Materials and Smart Living Laboratory, Department of Mechanical Engineering, University of Nevada, Las Vegas, Las Vegas, NV 89154, United States of America

² Department of Electrical and Computer Engineering, Michigan State University, East Lansing, MI 48824, United States of America

E-mail: kwang.kim@unlv.edu

Received 25 October 2021, revised 27 December 2021

Accepted for publication 24 January 2022

Published 7 February 2022



CrossMark

Abstract

The conductivity and dielectric properties are integral to the function of polyvinyl chloride (PVC) gel actuators. The frequency-dependent properties of PVC gel actuators are investigated here in terms of their impedance, permittivity, and for the first time, electric modulus. The data shows that PVC gels' conductive properties are just as, if not more, important as their dielectric properties in electromechanical transduction applications. The electrode polarization (EP) and its impact on the impedance and dielectric spectra of PVC gels, as well as the developed asymmetric space charge at the anode, are discussed. The electric modulus and $\tan \delta$ spectra are used for the fitting of Cole-Cole (CC) and Debye relaxation models for gels of varying plasticizer content. The electrostatic adhesive force for PVC gels of varying plasticizer is also measured, indicating large electrostatic adhesion ($>2 \text{ N cm}^{-2}$). A cyclic linear voltage sweep is used to clarify the dynamics of space charge within the gels. The peak current (associated with space charge development) is seen to be concurrent with the onset of mechanical deformation, showing the asymmetric charge as the origin of electromechanical transduction. Additionally, the maximum charge transferred (as measured by the integration of current over time) before space charge development is found to correlate with the electrostatic adhesive force measured for the gels, pointing to a new method of characterizing PVC gels for actuation.

Supplementary material for this article is available [online](#)

Keywords: PVC gel, soft robotics, dielectric actuator, artificial muscle, electric modulus

(Some figures may appear in colour only in the online journal)

1. Introduction

Polyvinyl chloride (PVC), typically an insulator, has been shown to have interesting electroactive properties upon adding

substantial amounts of ester-based plasticizers to form a gel. Electroactive polymers (EAPs) are polymer materials that perform electromechanical transduction; they have many possible applications as actuators in soft robotics for bio-applications and micro-electromechanical system devices, among others [1–3]. Dielectric elastomer actuators (DEAs) are one of the most studied EAP actuators and have been shown to be useful

* Author to whom any correspondence should be addressed.

in many applications [4, 5]. However, DEAs require high voltages (generally multiple kilovolts) to produce the high electric fields ($\sim 100 \text{ V } \mu\text{m}^{-1}$) that are necessary for appreciable mechanical motion [6]. While actuator materials with lower driving voltages such as conductive polymer actuators and ionic polymer-metal composites (IPMCs) exist, they are often plagued by reliability issues (with $<10^4$ maximum cycles) and require constant hydration [7–9]. PVC gels do not have these limitations. PVC gels are able to move in air, produce large strains, and have high response rates compared to alternative smart materials [10, 11]. PVC gel actuators exhibit large amounts of deformation and require lower driving voltages than DEAs as their deformation is localized within a thin layer at the anode surface [12]. This allows for PVC gels to be actuated in a variety of unique ways based upon the gel and electrode geometries, such as in contraction, bending, and varifocal lens applications [13–16]. This actuation mechanism is entirely unique to PVC gels; its fundamental principles have been the subject of much discussion and are not well understood at this time [17]. Current theories suggest that the space charge layer that is formed near the anode (confirmed by pulsed electroacoustic (PEA) measurements) is the cause of deformation [18, 19]. Impedance and broadband dielectric spectroscopy have been used to understand the polarization behavior of PVC gels [20, 21]. The primary focus has been on the bulk polarization of the materials with attempts to correct for the electrode polarization (EP) of the gels, as EP is generally considered a parasitic effect overshadowing the actual dielectric properties of the gel [20]. While useful to show that EP is indeed occurring, the correction of EP via a blocking sheet of polytetrafluoroethylene (PTFE) to shield the electrode and prevent electrical double layer formation does not enhance the permittivity data. Rather, it simply leads to Maxwell–Wagner polarization processes occurring between the two materials [22, 23]. The electric field experienced by the gel is also altered such that little useful information can be drawn from it. PVC gels are not simply dielectric actuators, and their actuation is not solely dependent upon dipole rotation processes. Early studies of PVC gels focused on the improved permittivity as a tangential qualitative metric for performance improvement, with increased relative permittivity being indirectly correlated with improved electromechanical actuation [24, 25]. More recent work has focused on utilizing the dielectric properties to inform electromechanical models, using the resistivity measurements to inform the electric field experienced in the anode adjacent layer and the permittivity measurements to inform the modeled layer thickness [21, 26, 27]. Other models of PVC gels have focused on using the measured impedance response and voltage-current relationship as feedback for control loops in PVC gel actuators [28, 29]. However, there is still a lack of focus in the literature on the conduction properties of PVC gels, which are essential for modeling and control of the time-dependent gel actuator response. The conductivity of the gels and the formation of EP are important components of the actuation of PVC gels, and the insights gained from the impedance spectroscopy are valuable for determining the effects of conductivity on the actuation of the gels.

While the permittivity plots are useful and have led to great insights into PVC gel behavior in previous studies, they fail to provide insight into the overall behavior in systems with mobile charges. Electric relaxation is commonly viewed through this frame, where the relaxation of the electric displacement field (\mathbf{D}), varies with an applied electric field (\mathbf{E}). However, the contribution of long-range mobile charges, and subsequent EP, suppress other relaxation processes [30]. For dielectrics that have mobile charges, such as PVC gels, viewing the relaxation of \mathbf{E} as a function of \mathbf{D} may be more appropriate and lead to insights not yet recognized in the case of plasticized PVC gel actuators [31]. This can be done through the use of the formalism of electric modulus, which works as a direct analogy to mechanical modulus in viscoelastic relaxation (with stress and strain being replaced by \mathbf{E} and \mathbf{D} , respectively) [32]. The electric modulus formalism allows for the spectral suppression of EP (as conductivity dispersion occurs at higher frequencies than EP relaxation) and adds new insight into the charge transport process characteristics within the gels.

In the present work, PVC gels with varying plasticizer ratios (1:0.5, 1:1, 1:2, 1:4, 1:6, 1:8 parts PVC to dibutyl adipate (DBA) by weight) are investigated. We aim to provide a more detailed look at the permittivity and conductivity properties of PVC gels, with a focus on the charge transfer process using the electric modulus formalism. The EP process is fit to Cole-Cole (CC) and Debye models for dielectric relaxation. The charge transfer within PVC gels at high voltage is analyzed through a cyclic linear voltage sweep and the results are compared with the mechanical deformation in both a bending actuator and a mesh contraction actuator. Lastly, the electrostatic adhesive force of the PVC gels is measured.

2. Methods

2.1. Materials and preparation of PVC gels

PVC gels were made from pure PVC powder ($M_w = 233\,000 \text{ g mol}^{-1}$, $M_n = 99\,000 \text{ g mol}^{-1}$), DBA ($M_w = 258.38 \text{ g mol}^{-1}$) plasticizer, and tetrahydrofuran (THF) solvent (with 20 ml of solvent/gram of PVC) purchased from Sigma-Aldrich Co. 1-part PVC was mixed with X-parts DBA plasticizer by weight (gels will be referred to as PX, e.g. P4, P6, P8, etc) at 30 °C for 24 h. The gels were then cast in a glass petri dish (10 cm diameter) and the THF was evaporated over 4 d at room temperature. The thickness of the PVC gels measured between 0.9 and 1.1 mm for all samples. The gels were then cut to specified size.

2.2. Spectroscopy measurements

Impedance spectroscopy measurements were used for characterization of the PVC gels' impedance, conductivity, and dielectric properties. Measurements were taken using an LCR meter (ET4510, East Tester) with an alternating current (AC), a frequency range of 10 Hz–100 kHz (5 points/decade), and a 1 V signal amplitude. The PVC gel samples (30 mm diameter)

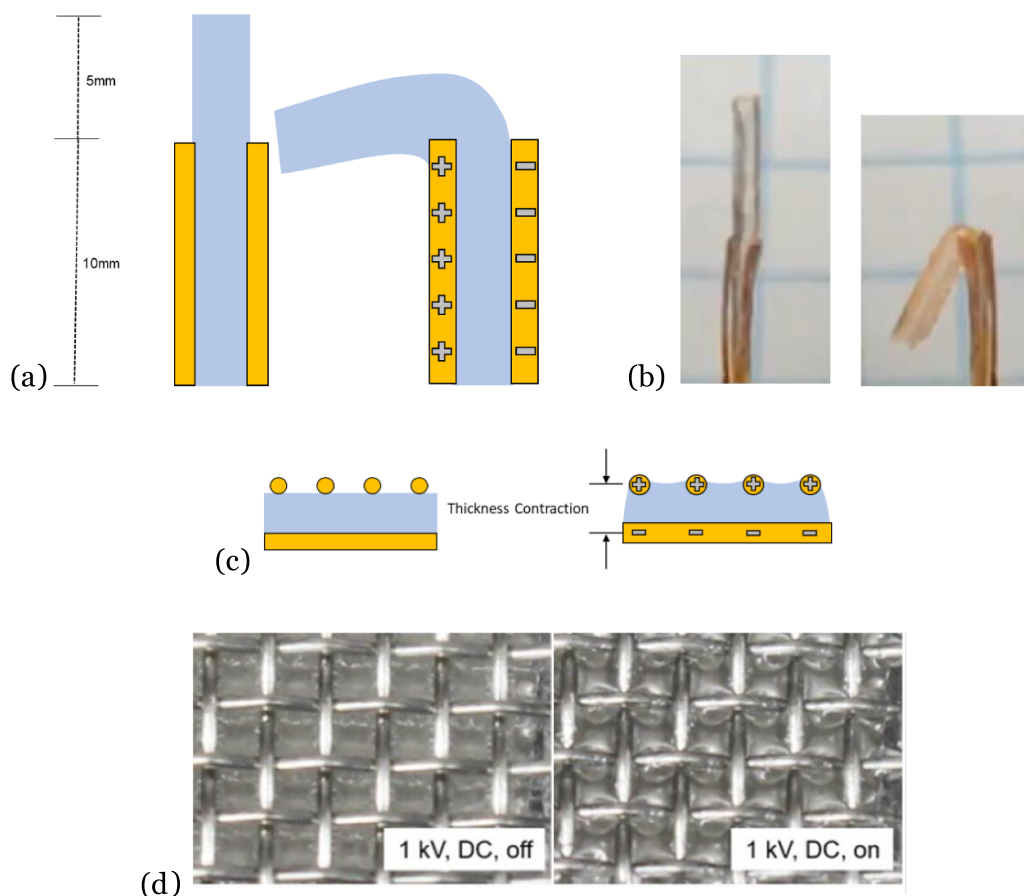


Figure 1. (a) PVC gel bending actuator before (left) and after (right) an applied voltage. (b) Photo of the same mechanism. (c) Contraction actuator before (left) and after (right) an applied voltage. (d) Top down view of a PVC gel contraction actuator without (left) and with (right) a 1 kV-DC electric field; the PVC gel demonstrates creeping deformation into the vacancies in the mesh causing contraction. Reproduced from [33]. CC BY 4.0.

were placed between two 25.4 mm (smaller than gel diameter to minimize capacitive edge effects) stainless steel parallel plate electrodes. A load cell was used to maintain consistent (low) contact force (supplementary S1 available online at stacks.iop.org/SMS/31/035020/mmedia).

2.3. Electrical and electromechanical response

The voltage input was produced with a signal generator (SDG-1025, Siglent Technologies), and high voltage amplifier (609×10^{-6} , TREK). The responses were analyzed using a data acquisition system (DAQ-6510, Keithley Instruments), and a load cell (GSO-100, Transducer Techniques) was used to ensure consistent force across samples (supplementary S2). Copper electrodes were used, and all measurements were taken at room temperature (17 °C). For the bending displacement response, a $15 \times 2 \times 1$ mm gel was sandwiched between two copper electrodes (with 10×2 mm² initial contact area). The contraction actuator utilized a copper foil cathode and mesh anode (100 wires/inch) as shown in figure 1. A laser displacement sensor was used to measure the displacement of the actuators (optoNCDT-1401, Micro-Epsilon).

2.4. Electrostatic adhesion force

The electrostatic adhesive force is measured by determining the force of detachment for a PVC gel placed in contact with two electrodes (test setup in supplementary figure S3). Due to the lack of electrostatic adhesion to the cathode (which experiences no electrode adjacent accumulation of charge and thus only initial contact adhesion), contact with the cathode is necessary to create a continuous injection of charges into the material to maintain the adhesive force at the anode. A holder which maintains the position and cathode contact is used. The gel is then loaded with increasing mass and slowly lifted (1 mm s^{-1}). This is repeated until detachment occurs and the load cell is recorded to determine the final adhesion strength of the PVC gels at a given voltage.

3. Results and discussion—electrical and electromechanical characteristics

3.1. Impedance spectroscopy

The AC complex impedance (Z^*) for PVC gels can be analyzed with electrochemical impedance spectroscopy (EIS) to

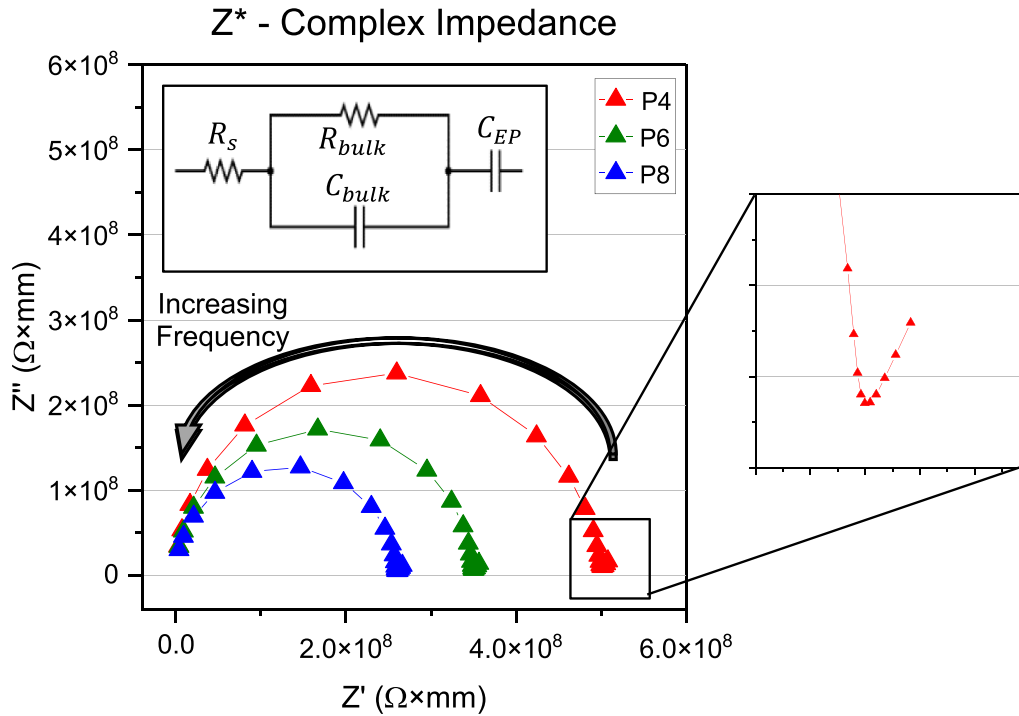


Figure 2. Argand plot for complex impedance for P4, P6, and P8 gels. (R_s , R_{bulk} , C_{bulk} , C_{EP} are the resistance of the electrodes, resistance and capacitance of the bulk gel, and the capacitance associated with the electrical double layer during EP.)

view their electrical behavior. This, along with the following sections covering the permittivity, electric modulus, and conductivity spectra of PVC gels will allow for quantitative description and analysis of their conduction and EP relaxation process. The Argand plot for PVC gels with varying plasticizer content can be seen in figure 2, which is a plot of Z^* in the complex plane with real (Z') and imaginary (Z'') components plotted as the x and y axes over a range of frequencies. The Z^* Argand plot for PVC gels has an inclined line at low frequencies with a semicircle intercepting the real impedance axis at higher frequencies. This PVC gel behavior, without bias voltage, can be fit to an equivalent circuit (figure 2 inset) which corresponds to an electrical double-layer capacitance at the interface between the gel and the electrodes (seen as the inclined line at lower frequencies), along with a parallel capacitance and resistance associated with the charge transport from the alternating electric field. There is also a series resistance which represents the electrode resistance at very high frequencies (offset of the real impedance of the semicircles from $Z' = 0$, although this is quite low compared to the overall impedance of PVC gels). From figure 2, P4 has the largest semi-circle diameter, with the size declining for increasing plasticizer content. This indicates an increasing conductivity with plasticizer content, as will be discussed later in section 3.4.

3.2. Permittivity spectra

The impedance measurements also allow for the determination of the dielectric properties of PVC gels. The relative permittivity (ϵ') of PVC gels is the real portion of the complex

permittivity (ϵ^*) and corresponds to the amount of charge that is stored within the gel via dipole interactions with the electric field. The dielectric loss (ϵ'') is the imaginary portion of ϵ^* and represents the energy lost within the material due to the alternating electric field, both by the resistance of dipoles to rotation and to the flow of charges through the material (direct current (DC) conduction). Both ϵ' and ϵ'' can be found from the frequency-dependent impedance through the relationships in equation (1):

$$\epsilon^* = \epsilon' - j\epsilon'' = \left(\frac{Z''}{\omega C_0 |Z|^2} \right) - j \left(\frac{Z'}{\omega C_0 |Z|^2} \right), \quad (1)$$

where ω is the angular frequency ($\omega = 2\pi f$), and C_0 is the free space capacitance ($C_0 = \frac{\epsilon_0 A}{d}$; A and d are electrode contact area and gel thickness, respectively). The comparison of relative permittivity and dielectric loss for PVC gels with varying plasticizer content can be seen in figure 3.

The permittivity of the PVC gels increases substantially at lower frequencies exhibiting low-frequency dispersion. The increase in ϵ' occurs at the same point as the inclined line seen in the Argand plot of PVC gel impedance (figure 2). Both the C-Cl on the PVC matrix chains as well as the Carboalkoxy (RCOOR') functional group in the adipate plasticizer are polar and contribute to the increased polarity of the overall gel. The relative permittivity of pure PVC is low (generally <4) and frequency-independent due to its rigidity preventing the rotation of its dipoles in an electric field. With the addition of plasticizer, the free volume within the gel is increased, resulting in a larger amorphous portion of the matrix and weakening of polymer chain crosslinks, facilitating free dipole rotation and

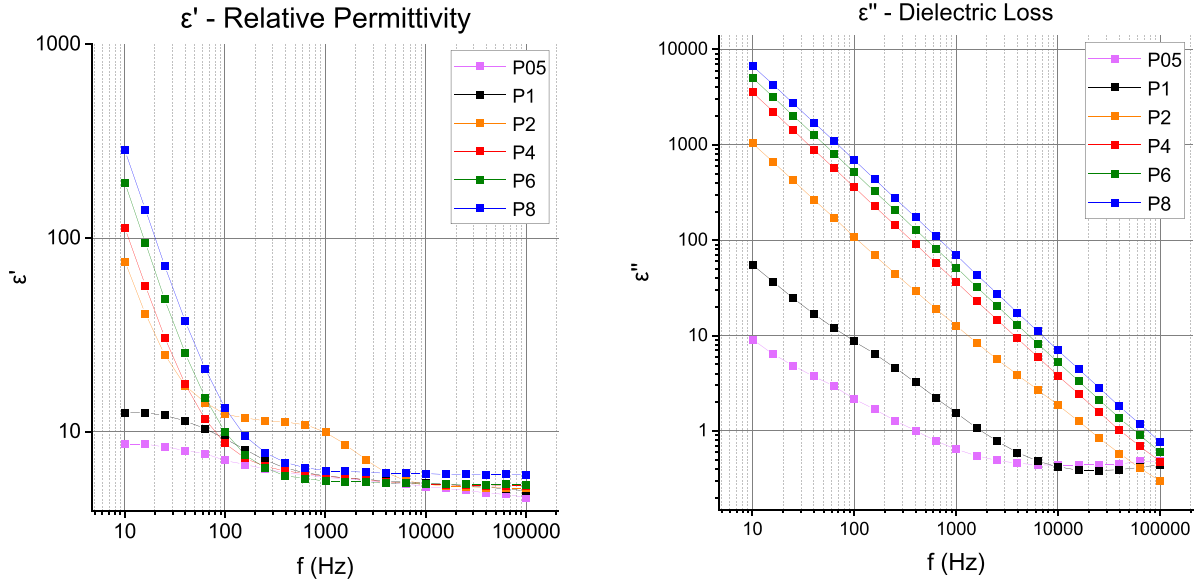


Figure 3. Permittivity comparison for PVC gels with varying plasticizer content; a transition behavior can be seen in the behavior of P2.

leading to an increased permittivity for the overall composite gel [34]. However, the extreme permittivity increase seen in PVC gels at lower frequency is not related to the dipole rotation of the PVC and DBA alone, but rather caused by EP (specifically near the anode), as has been confirmed by Ali *et al* through the measurement of the space charge distribution using the PEA method [20]. The EP is a result of charge migration through the PVC gel matrix as well as the segmental motion of the matrix itself. This behavior is specifically tied to the combinatory effects of the added liquid phase plasticizer. A transition can be seen in low plasticizer content plasticized PVC (P05, P1, and P2), from the relative permittivity behavior of the pure PVC, which is constant (and low) with regards to frequency, to the low-frequency dispersive behavior seen in PVC gels (P4, P6, and P8). The increase in the permittivity and dielectric loss is found to be dependent upon the amount of plasticizer, with increasing plasticizer content leading to higher permittivity and dielectric loss, this is due to the increased motion of charges (conductivity) brought on by the higher amorphous phase of the gel and lower attraction between the polymer backbone and the individual plasticizer molecules.

3.3. Electric modulus spectra

The dielectric properties of PVC gels have been studied in depth by multiple groups in the past, however the electric modulus of PVC gels has not [12, 21]. The electric modulus (M^*) is the inverse of ϵ^* . While the same information is technically present in both plots, the use of electric modulus allows for the identification and analysis of the relaxation of conductive charges, which is not easily seen in the ϵ^* spectra alone. The complex-valued electric modulus is defined as equation (2)

$$M^* = \frac{1}{\epsilon^*} = \frac{\epsilon'}{(\epsilon'^2 + \epsilon''^2)} + \frac{j\epsilon''}{(\epsilon'^2 + \epsilon''^2)} = M' + jM'' \quad (2)$$

with real and imaginary parts M' and M'' , respectively. The conductivity relaxation frequency (ω_m) occurs at the maximum of M'' , giving the most probable conductivity relaxation time (τ_M) [35]. When $f > f_{\max}^Z$, the charge transport is dominated by local short-range motion, as the charges move only via trap-controlled hopping between localized potential wells, and the C–Cl and C=O dipoles are unable to fully orient themselves in the direction of the field before the polarity of applied voltage reverses.

Comparing M'' and Z'' (as defined in equations (3) and (4), respectively), M'' can be related to the long-range electric relaxation of the material, while Z'' is related to the local relaxation of dipolar entities

$$M'' = Z' \left(\frac{\omega \epsilon_0 A}{d} \right) \quad (3)$$

$$Z'' = \epsilon' |Z|^2 \left(\frac{\omega \epsilon_0 A}{d} \right) \quad (4)$$

When $f < f_{\max}^{M'}$ the charges have time to migrate through the material and the long-range motion of charges occurs.

The fact that there is only a small shift in ω_m with increasing plasticizer content beyond P4 implies that the long-range electric relaxation mechanism in P4–P8 is not significantly altered and there is very little conductivity dispersion (only one relaxation time exists), irrespective of further increases in plasticizer content. This is not however the case for P1 gel, where we see that ω_m is significantly shifted towards lower frequencies in comparison to the higher plasticizer content PVC gels. Comparing the peak for P1 versus P4–P8 significant broadening is visible (more easily seen in the normalized graph of M'' and $\log(\omega)$ in figure 4), which indicates a large deviation from Debye-relaxation (for which the full width at half-maxima is 1.144) and a range of relaxation times within

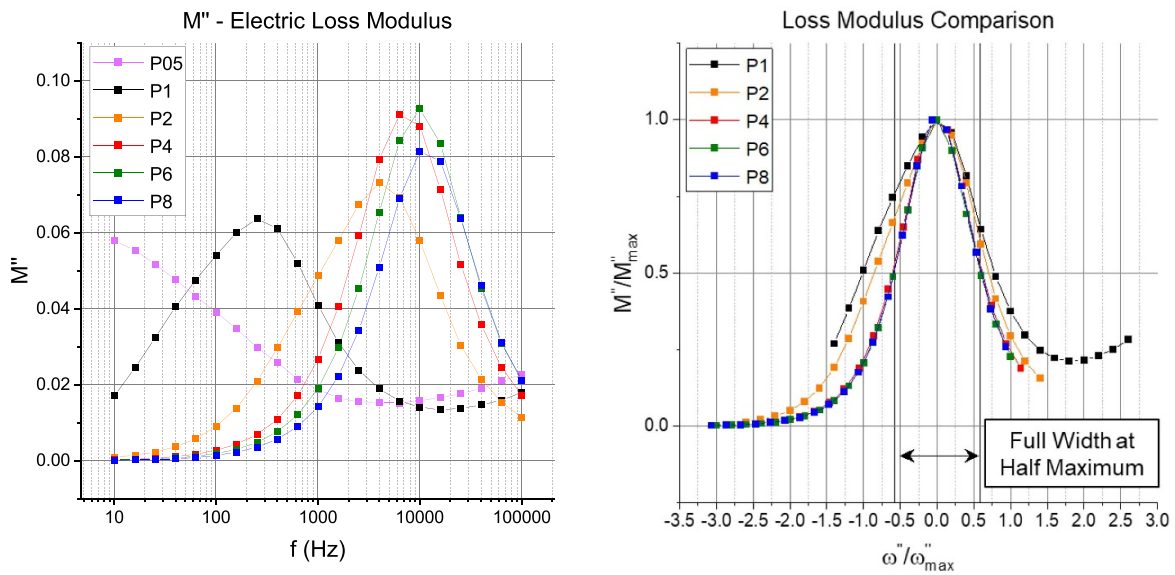


Figure 4. (Left) Electric loss modulus M'' comparison; varying plasticizer content; (right) M'' normalized to frequency peak.

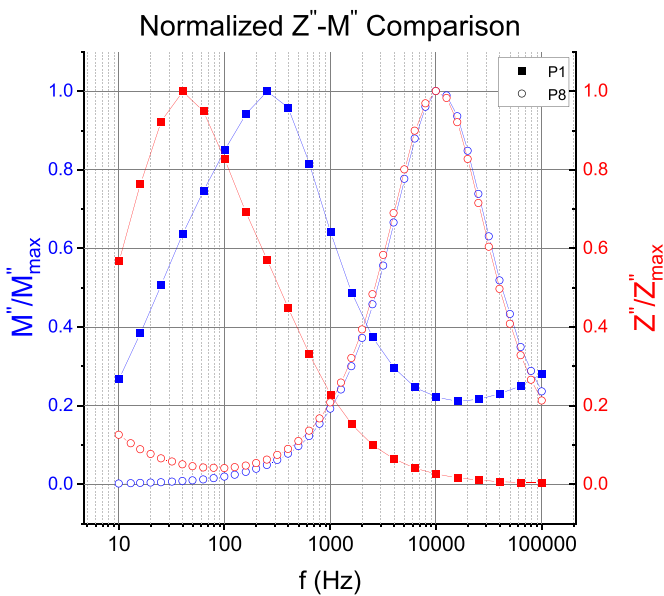


Figure 5. Normalized Z'' - M'' ; P1—closed markers, P4—open markers.

the material [36]. It is also possible to see this transition by looking at the overlap of the normalized M'' and Z'' spectra for P1 and P8 (figure 5). For PVC gel systems (P4–P8), the M'' and Z'' curves (and underlying relaxation processes) can be seen to follow the same curve, with $f_{max}^{M''} \approx f_{max}^{Z''}$. This is not the case for all systems with mobile charges in general (and in fact it can be seen from P1 that it is not the case in low plasticizer PVC gels either) and indicates that the long range motion of charges is the dominant form of charge transfer within PVC gels as opposed to localized motion. Note that $f_{max}^{Z''} \leq f_{max}^{M''}$,

will always hold; larger differences between the two indicates the dominance of localized charge hopping as the mechanism for conduction in P05–P2 [37]. The overlap in P4–P8 gels in figure 5, and the narrow peak (FWHM ≈ 1.144) in figure 4, also indicates that the EP process in these gels can be viewed as a Debye-like relaxation. This means that the addition of plasticizer allowed for facile conduction through the gels that is not possible for simply plasticized PVC (such as P05 and P1). With the addition of enough plasticizer, the process can be viewed as a conductive one rather than a purely dielectric one. The electric modulus formalism provides a new view of the conduction and dielectric polarization process within the gels and is a more explicit illustration of the transition behavior with increasing plasticizer content, which was previously only able to be loosely understood by looking at the permittivity alone.

3.4. Conductivity spectra

The DC and AC conductivities (σ_{DC} and σ_{AC} , respectively) of the gels were analyzed to determine the steady-state and transient conductivity behavior of the PVC gels. The conductivity of the gels has two parts, the first being related to the DC conductivity of the gels which is frequency-independent, and the second part being a frequency-dependent portion. The plateau of the conductivity versus frequency curves (figure 6), is equal to σ_{DC} . Above this plateau the conductivity can be seen to be exponentially dependent upon frequency, with the frequency-conductivity relation being described by Jonscher's power law [38]:

$$\sigma_{AC}(\omega) = \sigma_{DC} + B\omega^s, \quad (5)$$

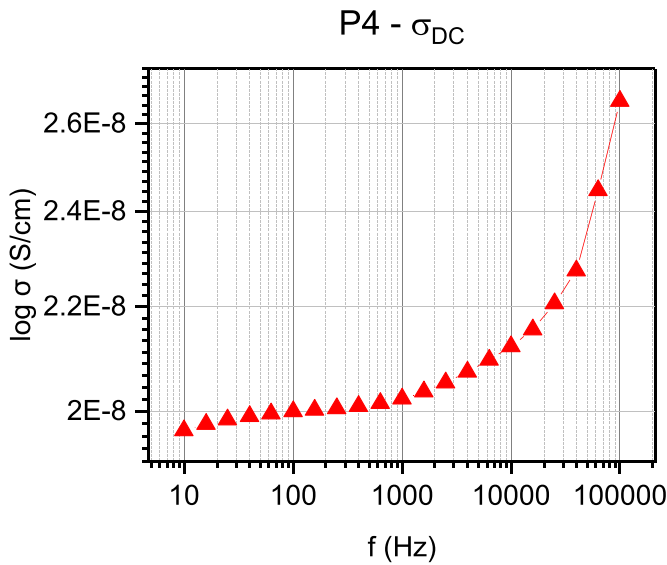


Figure 6. Sample conductivity plot for P4 gel.

where σ_{AC} is the frequency-dependent AC conductivity, B is a pre-exponential constant, ω is the angular frequency ($2\pi f$), and s is a power law exponent ($0 < s < 1$).

σ_{DC} can also be seen visually as the diameter of the semi-circle formed by the low and high frequency intercept of Z^* with the real impedance axis (where Z'' reaches a local minimum). Additionally, the dielectric loss for the materials at low frequencies can also be seen to follow a similar response, with a nonlinear dependence on the measurement frequency as seen in equation (6)

$$\varepsilon''(\omega) \propto \omega^{n-1}. \quad (6)$$

The electrical properties of the gels studied can be seen in table 1. For n , the closer the values are to approaching 1, the more accurately the relaxation approximates Debye relaxation. P1 is seen to have over 2 orders of magnitude lower conductivity than P4 and note that the conductivity of P4 gels is also 4 orders of magnitude greater than is typical for pure PVC. Below the frequency range measured here (<10 Hz), it has been reported that the conductivity of PVC gels shows a steep decrease related to the increasing charge buildup and EP at the gel-electrode interface, as is common in systems with mobile charges, only the start of this process can be seen here in the conductivity spectra of the gels at lower frequencies [39].

3.5. Cole-Cole and Debye fitting

The dielectric loss tangent, $\tan(\delta)$ is an easier relaxation to see in the current spectrum than ε'' as it suppresses conductivity, and the peak maximum is shifted to a frequency in the measured range. The relaxation observed in the permittivity spectra is related to the EP of the material. The $\tan(\delta)$ corresponding to this polarization process can be fit with a CC equation, as seen in equation (7) [40–42]. Equation (7) can also be separated into real and imaginary components, resulting in equations (8) and (9), respectively

$$\varepsilon_{EP}^* = \varepsilon_r + \frac{\varepsilon_{EP} - \varepsilon_r}{1 + (j\omega\tau_{EP})^{1-\alpha}} \quad (7)$$

$$\varepsilon' = \varepsilon_r + \frac{1}{2}(\varepsilon_{EP} - \varepsilon_r) \left[1 - \frac{\sinh((1-\alpha)x)}{\cosh((1-\alpha)x) + \sin\left(\frac{\alpha\pi}{2}\right)} \right] \quad (8)$$

$$\varepsilon'' = \frac{1}{2}(\varepsilon_{EP} - \varepsilon_r) \frac{\cos\left(\frac{\alpha\pi}{2}\right)}{\cosh((1-\alpha)x) + \sin\left(\frac{\alpha\pi}{2}\right)} \quad (9)$$

$$\tan \delta = \frac{\varepsilon''}{\varepsilon'} \quad (10)$$

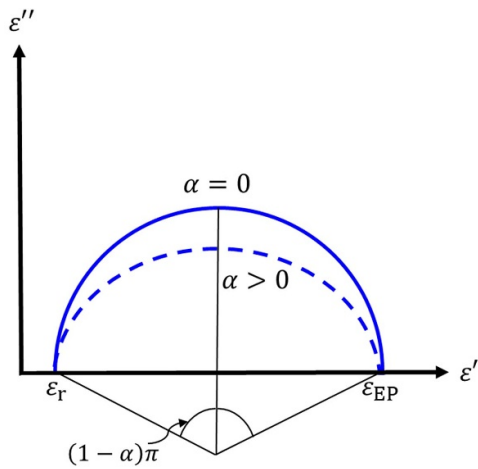
ε_{EP}^* is the frequency-dependent permittivity associated with the EP process, ε_{EP} is the low frequency value of the measured relative permittivity, ε_r is the high frequency value of ε' , while τ_{EP} is the time constant associated with the EP process (x is equal to $\ln(\omega\tau_{EP})$). The exponential fitting parameter for the CC equation, α , is indicative of how close a given process is to true Debye relaxation (where $\alpha = 0$ for Debye relaxation). The diagram in figure 7, shows a perfect Debye relaxation compared to a CC relaxation. The fitting parameter α , and how it relates to the depression of the semicircle seen in the ε^* spectra can also be seen.

It has previously been reported that the EP process of PVC gels prevents the fitting of a relaxation model, as the permittivity does not seem to have the semi-circular shape expected for Debye-like relaxations [20]. The reason for this is that the EP time constant, τ_{EP} , falls well outside of the range that is generally measured for broadband impedance spectroscopy. Given this, when looking at a proper CC plot (wherein the axes are of equal sizing such that a semi-circle appears appropriately), it can easily seem as though the permittivity data produces a nearly vertical line. However, figure 8 shows that the polarization can be fit with a CC model and that the full relaxation semi-circle (figure 8 inset) is much larger than one would initially expect from a standard dielectric relaxation, leading to this misconception. It should be noted that the relaxation is not a dielectric orientation process, but rather a function of charge transfer within the gel, so in terms of the 'true' bulk permittivity the original assertion is still correct; however, that is not the primary concern in the case of PVC gel actuators. The alternative method, using a blocking sheet of PTFE, does not enhance the permittivity data as it simply leads to a Maxwell–Wagner polarization processes occurring between the two materials and the electric field experienced is also altered such that no useful information can be drawn from it [22].

The α value obtained for $\tan(\delta)$ fit is extremely small for P4–P8 gels, indicating a Debye-like fit. The primary issue with the use of $\tan(\delta)$, however, is that the measurement uncertainty at the high values seen in P4–P8 gels is quite large (as a small change in the measured impedance phase angle θ leads to a very large change in $\tan(\delta)$). The $\tan(\delta)$ plot for P0.5–P8 gels with uncertainty can be seen in figure 9. Given this, not much can be said about the differences in $\tan(\delta)$ between P4–P8 gels, beyond the fact that as a group they have a more uniform relaxation than P05–P1 gels and a transition can be

Table 1. Electrical property summary of PVC gels.

Gel	σ_{DC} (S cm ⁻¹)	$\omega_{\max}^{\tan\delta}$ (Rad s ⁻¹)	$\tan(\delta)_{\max}$	τ_{EP} (s)	ε_{EP}	τ_M (s)	α	n
P1	2.95×10^{-10}	Out of range	Out of range	Out of range	6.9×10	7.79×10^{-4}	0.269 For M'' fit only	0.753 ± 0.006
P2	5.25×10^{-9}	116	16.9	0.32	2.21×10^4	4.99×10^{-5}	0.010 3	0.889 ± 0.009
P4	2.01×10^{-8}	220	50.7	0.66	1.43×10^5	2.30×10^{-5}	4.8×10^{-3} For $\tan\delta/CC$ fit	0.978 ± 0.004
P6	2.85×10^{-8}	331	54.0	0.48	1.68×10^5	1.64×10^{-5}	4.6×10^{-3} For $\tan\delta/CC$ fit	0.988 ± 0.002
P8	3.84×10^{-8}	409	52.1	0.42	2.03×10^5	1.38×10^{-5}	5.2×10^{-3} For $\tan\delta/CC$ fit	0.991 ± 0.001

**Figure 7.** Diagram of Debye polarization ($\alpha = 0$) and CC polarization depressed semicircle indicative of a symmetric distribution of relaxation times ($\alpha > 0$).

seen in the P2 $\tan(\delta)$ spectrum. The uncertainty in the measurement of the electric modulus however is much lower (as it is performed at higher frequencies and values of the phase shift θ are higher) and can also be fit with the CC equation (equation (11)), and the conductivity dispersion time can also be related to the polarization time and permittivity ratio as seen in equation (12) (full derivation of CC in M^* spectra in supplementary) [32].

$$M^* = M_\infty - \frac{M_\infty - M_{EP}}{1 + (j\omega\tau'_M)^{1-\alpha}} \quad (11)$$

$$\tau'_M = \left[\tau \left(\frac{\varepsilon_r}{\varepsilon_{EP}} \right)^{\frac{1}{1-\alpha}} \right] = \tau_M \left[\left(\frac{\varepsilon_r}{\varepsilon_{EP}} \right)^{\frac{\alpha}{1-\alpha}} \right] \quad (12)$$

where M_∞ is the electric modulus at high frequencies, when only short-range localized conduction is present (i.e. $M_\infty = \frac{1}{\varepsilon_r}$), M_{EP} is the electric modulus after EP (i.e. $M_{EP} = \frac{1}{\varepsilon_{EP}}$), and τ'_M is a modified conductivity relaxation time for relaxations that are better fit by the CC equation as opposed to a Debye relaxation ($\alpha = 0$). In the case of P4–P8 gels, the peaks

were able to be sufficiently described by a Debye distribution ($\alpha \approx 0$) i.e.

$$M^* = M_\infty - \frac{M_\infty - M_{EP}}{1 + (j\omega\tau_M)} \quad (13)$$

$$\tau_M = \tau_{EP} \left(\frac{\varepsilon_r}{\varepsilon_{EP}} \right) \quad (14)$$

The loss tangent can be viewed as a function of the ratio of frictional energy of charge transfer to the thermal energy of the gel as it is a function of the Debye layer thickness (derivation in supplementary) [43]:

$$(\tan\delta)_{\max}^2 \propto \frac{d}{2\lambda_d} \propto \frac{D\eta}{k_B T} \text{ or } \left[\frac{U_{\text{friction}}}{U_{\text{thermal}}} \right]. \quad (15)$$

Note that this analysis only applies when the peak is Debye-like, and that, while the correlation may exist for P05–P2, the derived relation in equation (15) does not apply very well to lower plasticizer content materials (P05–P2) which have a substantial distribution of relaxation times (as analyzed from the M'' peak comparison in figure 4) in the gel leading to a much broader and less distinct peak. Increasing plasticizer content of the gels leads to a decrease in the relaxation times of the material (faster motion of charges) and also a decrease in the double layer thickness, indicating an increased frictional resistance to charge motion. Material properties and dielectric fitting parameters can be seen in table 1.

3.6. Cyclic linear voltage sweep

The current of PVC gels was monitored with a linear varying electric potential to analyze the effects of sweep rate on the current response. The voltage applied to a PVC gel in a parallel plate configuration was linearly swept from -500 V up to 500 V and back down. The effect of varying the voltage scan rate can be seen in figure 10.

The I – V curve is linear up to a point where the current can be seen to form a distinct peak at a specific voltage before rapidly declining. This is due to the charges, which are initially polarized at one electrode, taking a substantial amount of time to migrate towards the opposite electrode after a polarity reversal. The current peak can be seen to shift to a higher

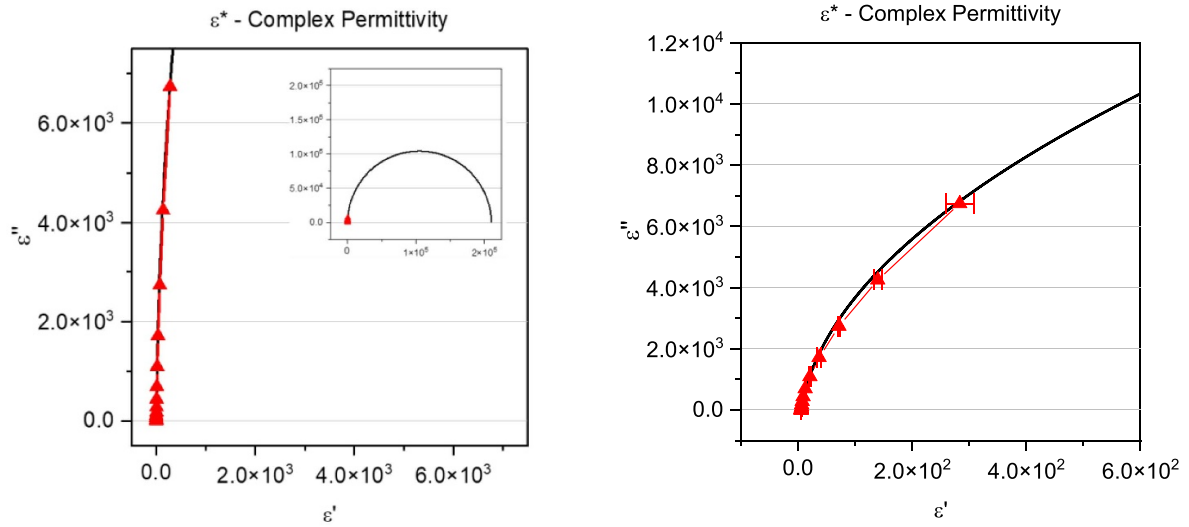


Figure 8. (Left) CC Plot for P8 gel with CC fitting. (Left Inset) Zoomed out version of the same plot to see the entire modeled line. (Right) Scaled ε^* plot for optimal visibility of fitting and values.

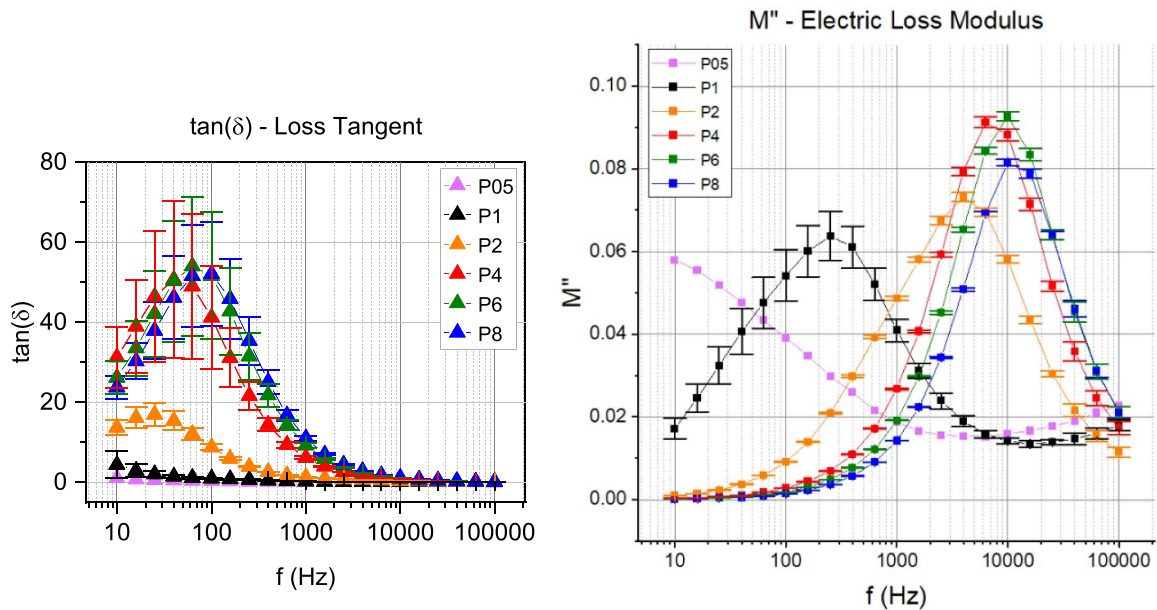


Figure 9. (Left) $\tan(\delta)$ comparison for gels with varying plasticizer content with error bars. (Right) Electric loss modulus (with error bars).

current (and voltage) value with an increasing voltage scan rate (figure 10 and table 2). However, the total charge transferred (calculated from equation (16)) was found to be constant for a given PVC gel, indicating that the amount of charge moving through the gel upon subsequent sweeps was unchanged by the scan rate. This means that after the first scan (where initial charge injection occurs at high voltages), the number of charge carriers in the gel remains relatively unchanged. Additionally, the charge stored was also found to be negatively correlated with the maximum loss tangent for the PVC gels, with P6 storing the least amount of charge

$$Q = \frac{1}{A} \int_{t_{\text{peak}}}^{t_{0v}} idt. \quad (16)$$

The leakage current of the system can be compensated for through the dynamic leakage current compensation method [44]. The current measured at adjacent frequencies can be used to compensate for the leakage current (which should be independent of the voltage scan rate), to separate it from the current due to capacitance and charge migration (which is taken to be linearly dependent upon frequency as a first approximation).

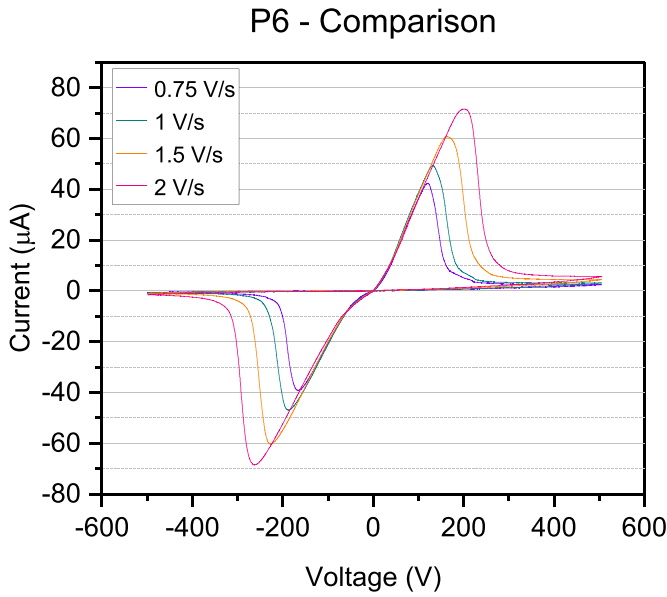


Figure 10. I - V plot for the response of a P6 gel to cyclic linear voltage sweep for varying sweep rates.

Table 2. P6 cyclic linear voltage sweep peak properties.

Scan rate $V s^{-1}$	$i_{peak} \mu A$	$V_{peak} V$	$Q mC cm^{-2}$
0.75	42.5	120.5	2.53
1.0	49.4	132.9	2.50
1.5	60.8	163.1	2.56
2.0	71.6	192.5	2.84

This can be combined with the switching of bipolar and unipolar waveforms to determine the coercive voltage and to separate the current caused by charge migration and space charge accumulation from the capacitance and leakage current

$$i_{total} = i_R + i_c(\omega) + i_{switch}(\omega) \quad (17)$$

$$i_c(\omega) = V * (j\omega C), \quad (18)$$

where i_R is the leakage current associated with the DC resistivity of the material, i_c is the current read as a result of bulk capacitive effects in the gels, and i_{switch} is the current from space charge transfer between the electrodes. The frequency dependence of i_c and i_{switch} , allow for the current to be rewritten as equation (19), and the difference between the two frequencies can be found to be equation (20) and used to find the compensated current for ω_1

$$i_{total}(\omega) = i_R + \omega i_C^0 + \omega i_{switch}^0 \quad (19)$$

$$\Delta i = (\omega_2 - \omega_1) (i_C^0 + i_{switch}^0) \quad (20)$$

$$i_{comp}(\omega) = \frac{\omega}{\omega_2 - \omega_1} [i(\omega_2) - i(\omega_1)], \quad (21)$$

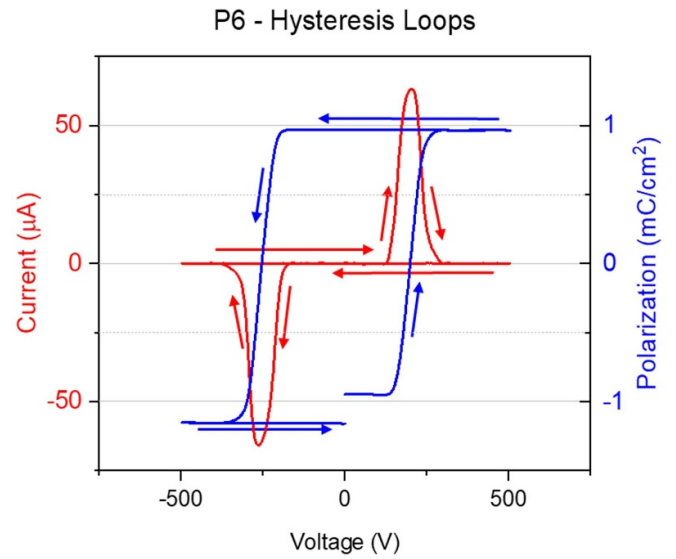


Figure 11. Compensated I - V and P - V plots for P6 at $1 V s^{-1}$.

where i_C^0 and i_{switch}^0 are frequency independent constants corresponding to i_C and i_{switch} , respectively. When $\omega_2 = 2\omega_1$, the compensated current equation simplifies to equation (22)

$$i_{comp}(\omega_1) = (\omega_1) (i_C^0 + i_{switch}^0). \quad (22)$$

The compensated current removes the leakage current effects from the system, allowing for determination of the polarization change within the material (i.e. through dielectric polarization and the motion of space charge throughout a cycle). The peak polarization value may be able to be used as a proxy for direct measurement of space charge in the gels, but this will be left to future studies. The compensated current for P6 gels with $1 V s^{-1}$ can be seen in figure 11. The maximum transferred charge between different scan rates is nearly identical, but the peak current and the coercive voltage at which the peak current occurs have increased with the increasing scan rate. The polarization value here can be thought of as the maximum polarization of the material from its initial electrostatically neutral state where no electric field is applied. The total charge present should be equal to the magnitude of the space charge layer that is developed at the anode, which is the primary driver of PVC gel actuation. This method provides a simple way to find an easily measurable scalar value associated with the total polarization of the gels, but with a much easier and less costly process than the direct measurement of space charge through Pulsed Electroacoustic (Method) PEA or similar methods.

A $1 kV-1 V s^{-1}$ linear voltage sweep for PVC gels was performed while measuring the displacement of both a bending actuator between parallel plate electrodes (figure 12) and a contraction actuator utilizing a mesh anode and plate cathode (figure 13).

In the case of the bending actuator, the takeaway is quite clear. The actuator is initially at rest as the charge is moved through the gel, and then upon reaching the electrode the current is seen to peak at the exact time that bending actuation begins. The peak tip displacement occurs at the $1 kV$ voltage

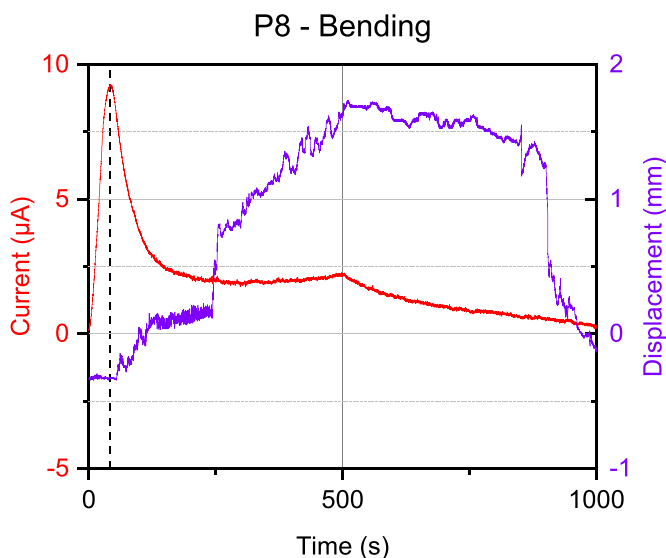


Figure 12. $I-t$ and $x-t$ plots for a bending actuator with a $1 \text{ kV} = 1 \text{ V s}^{-1}$ voltage sweep.

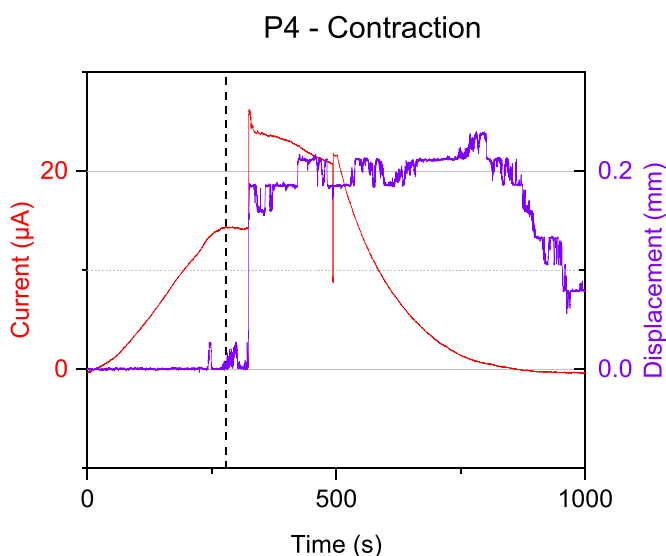


Figure 13. $I-t$ and $x-t$ plots for a mesh contraction actuator with a $1 \text{ kV} = 1 \text{ V s}^{-1}$ voltage sweep.

peak before declining with the voltage ramp on the way back down.

Similarly, in the case of the mesh contraction actuator, the current can be seen to increase linearly until it peaks, and deformation begins. However, in the case of the mesh contraction actuator, the sudden deformation leads to a rapid increase in the anode contact area. This can be seen as a large spike in the current followed by the expected decline.

These plots show that the peak current during the linear sweep corresponds to the onset of actuation within the PVC gels, before the switching polarization no actuation is seen, and when the linear scan rate is too high the gels fail to actuate (despite technically being well above their traditional actuation frequency as described for unipolar actuation with a DC voltage). This is evidence of the following theory: prior to the

actuation of the gels, the electrical energy is almost entirely lost to the movement of charges through the gel (conduction), only once the charge has reached the opposite electrode and formed a layer of space charge can the gel actuate. Therefore, any model that seeks to describe the full electromechanical transduction of PVC gels, needs to account for not only the complex actuation of the gels with the assumption of a space charge region which has already formed a distinct DBA rich layer (as has been described in various studies) but also for the history-dependent hysteresis of the gels actuation [21, 27, 45]. This is particularly important in applications where the gel might be usefully actuated in multiple directions such as a multi-directional bending actuator [14].

3.7. Electrostatic adhesion

To study the effects of the unique mechanism of PVC gels, the electrostatic adhesive strength of PVC gels was tested. Electrostatic adhesion originates from the coulombic force between either two electrodes or, more commonly for most applications, an electrode and an initially neutral substrate [46]. In the most common configuration, two flat electrodes are placed side by side and separated from each other and the substrate by an insulator. An AC voltage applied (switching between the two). This induces charges on the surface and allows for an attractive force to maintain contact between the two surfaces. In the case of PVC gels, however, the accumulation of negative charges within the PVC gels near the anode creates an attractive force to the opposing positive charges on the conductive electrode surface. The electrostatic adhesive force only occurs on the anode due to the asymmetric formation of space charge near it in comparison to the cathode. The PVC gels have an initial tackiness that increases with plasticizer content and has been subtracted from the overall force measured in the electrostatic adhesion measurements reported. This mechanism of electrostatic adhesion allows for high forces at low voltages to be achieved, but also limits the use of PVC gels to conductive substrates.

The electrostatic adhesion force (figure 14) shows a large increase above approximately 200 V, and quickly begins to level off after. This is believed to be caused by a large amount of energy being stored with initial increases in voltage, with a screening effect occurring at higher voltage values leading to the asymptotic maximum electrostatic adhesion observed. A sharp transition can be seen to occur within the gels from P1 to P2, with P1 having very low adhesion and P2 having the highest of the unmodified gels. This is believed to be due to the fact that in P1 an insufficient amount of charge is able to be transferred to form an effective space charge layer due to the low conductivity of the gel. P2 gels are also where the mole ratio of the primary functional groups in PVC (C-Cl) and DBA (RCOOR') is ~ 1 (mole ratios available in the supplementary). Whether this particular correlation is relevant to the ability of charges to move through the gel and develop a space charge will be the subject of further study.

The correlation of the electrostatic adhesion in the gels with the measured charge transferred before space charge development (table 3) points towards the measurement of coercive

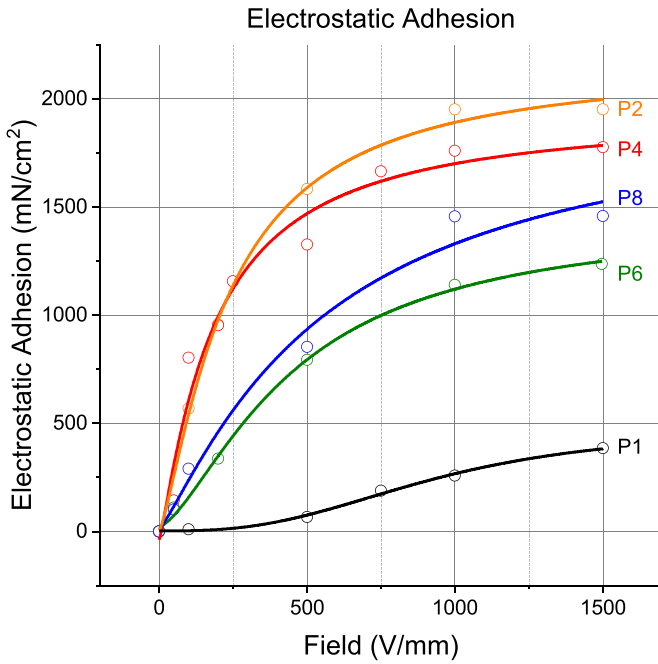


Figure 14. Electrostatic adhesion force with varying voltages for P1–P8 gels.

Table 3. Cyclic linear voltage sweep comparison by plasticizer content.

Gel	$i_{\text{peak},0.75 \text{ V s}^{-1}} \mu\text{A}$	$V_{\text{peak},0.75 \text{ V s}^{-1}} \text{V}$	$Q_{\text{avg}} \text{mC cm}^{-2}$
P4	45.0	146	3.74 ± 0.20
P6	42.5	133	2.55 ± 0.16
P8	47.4	155	3.52 ± 0.15

voltage through a linear voltage sweep as a novel method for electromechanical characterization of PVC gels. The electrostatic adhesion force may be described similarly to that of the electrostatic force (derived by Izadi *et al*) used by geckos that occurs during contact electrification. In the case of PVC gels, however, the charge density is generated from the flow of current and space charge formation with an applied voltage rather than by contact electrification phenomenon [47]

$$f_{\text{ES}} = -\frac{A\sigma_s^2}{2\varepsilon_0\varepsilon_{r,\text{eq}}} \quad (23)$$

$$\frac{d_{\text{air}} + d_{\text{SCL}}}{\varepsilon_{r,\text{eq}}} = \frac{d_{\text{air}}}{\varepsilon_0} + \frac{d_{\text{SCL}}}{\varepsilon_r}, \quad (24)$$

where f_{ES} is the electrostatic adhesive force, σ_s is the surface charge density, A is the anode contact area, d_{SCL} is the space charge layer thickness, and d_{air} is the thickness of the air gap between the gel and the electrode. This explanation can account for the correlation found between electrostatic force and the charge transfer polarization found in section 3.6, and with space charge as reported by Ali *et al* [48]. The air gap in the case of PVC gels is expected to be almost negligible due to the compliance of the soft gel surface. This would mean that the space charge layer and the permittivity of the

material are the primary controllable variables for optimization of PVC gels' electrostatic adhesion force. Some applications of the electrostatic adhesion described here could include a compliant electrostatic chuck, a combined gripper (utilizing anodophilic bending actuators in conjunction with electrostatic adhesion), and wall climbing robots.

4. Conclusion

Herein, the conductivity and dielectric characteristics of PVC gels were investigated. The electric modulus formalism was applied to PVC gel impedance data for the first time, and the long-range motion of charges was shown to be the dominant conductive process within PVC gels through the normalized M'' and Z'' relaxation curves. The modulus and $\tan(\delta)$ show significant sharpening of their peaks with increasing plasticizer content, indicating a smaller distribution of relaxation times and Debye-like conductivity relaxation behavior. The $\tan(\delta)$ spectra were used to fit CC plots for the EP process, and for P4–P8 gels the M'' spectra were utilized to fit a Debye relaxation curve in order to determine the characteristic polarization and conductivity relaxation times. These are critical for understanding the actuation response times of PVC gels, both in unidirectional applications (where a voltage is repeatedly applied to the same electrode) and in future multidirectional applications (such as in multidirectional bending with polarity reversal). A cyclic linear voltage sweep was run on various PVC gels, and a switching current peak was found corresponding to the charges in the gel reaching the opposite electrode. The onset of actuation was found to correlate directly with the peak, indicating that the electrical energy upon polarity reversal is initially lost to charge migration (conductivity), and only once the space charge has reached the anode and formed a layer of increased charge density does electromechanical transduction and subsequent actuation occur. The peak electrostatic adhesive force for P1–P8 gels was found to be correlated with the peak charge transferred during the linear voltage sweep as well as the maximum $\tan(\delta)$, indicating that a linear voltage sweep may be used as a possible method for electromechanical characterization of PVC gels.

Data availability statement

The data that support the findings of this study are available upon reasonable request from the authors.

Acknowledgments

Z F and K J K acknowledge the partial financial support from the US National Science Foundation (NSF), Partnerships for International Research and Education (PIRE) Program, Grant No. 1545857. Any opinions, findings and conclusions or recommendations expressed in this material are those of the author(s) and do not necessarily reflect the views of the NSF. Also, this work was, in part, supported by the Department of Energy Minority Serving Institution Partnership Program

(MSIPP) managed by the Savannah River National Laboratory (SRNL) under SRNS contract TOA# 0000525180. Additionally, K J K and J N extends their special thanks to Vivian Holloway of SRNL for encouragement.

ORCID iDs

Zachary Frank  <https://orcid.org/0000-0002-3567-406X>

Mohammed Al-Rubaiai  <https://orcid.org/0000-0003-2335-0196>

Kwang J Kim  <https://orcid.org/0000-0003-2134-4964>

References

- [1] Carpi F 2016 *Electromechanically Active Polymers* (Springer International Publishing)
- [2] Bar-Cohen Y 2005 Electroactive polymers as artificial muscles—reality and challenges *Proc. SPIE, Smart Structures and Materials: Electroactive Polymer Actuators and Devices (EAPAD) 2005*
- [3] Palmre V, Pugal D, Kim K J, Leang K K, Asaka K and Aabloo A 2014 Nanothorn electrodes for ionic polymer-metal composite artificial muscles *Sci. Rep.* **4** 1–10
- [4] Hwang T, Kwon H-Y, Oh J-S, Hong J-P, Hong S-C, Lee Y, Ryeol Choi H, Jin Kim K, Hossain Bhuiya M and Nam J-D 2013 Transparent actuator made with few layer graphene electrode and dielectric elastomer, for variable focus lens *Appl. Phys. Lett.* **103** 023106
- [5] Araromi O A, Rosset S and Shea H R 2015 High-resolution, large-area fabrication of compliant electrodes via laser ablation for robust, stretchable dielectric elastomer actuators and sensors *ACS Appl. Mater. Interfaces* **7** 18046–53
- [6] Xiang D, Liu L and Liang Y 2017 Effect of hard segment content on structure, dielectric and mechanical properties of hydroxyl-terminated butadiene-acrylonitrile copolymer-based polyurethane elastomers *Polymer* **132** 180–7
- [7] Shahinpoor M, Bar-Cohen Y, Simpson J O and Smith J 1998 Ionic polymer-metal composites (IPMCs) as biomimetic sensors, actuators and artificial muscles—a review *Smart Mater. Struct.* **7** R15–R30
- [8] Shahinpoor M and Kim K J 2001 Ionic polymer—metal composites: I. Fundamentals *Smart Mater. Struct.* **10** 819–33
- [9] Santaniello T, Migliorini L, Borghi F, Yan Y, Rondinini S, Lenardi C and Milani P 2018 Spring-like electroactive actuators based on paper/ionogel/metal nanocomposites *Smart Mater. Struct.* **27** 065004
- [10] Xia H, Ueki T and Hirai T 2011 Direct observation by laser scanning confocal microscopy of microstructure and phase migration of PVC gels in an applied electric field *Langmuir* **27** 1207–11
- [11] Uddin M Z, Watanabe M, Shirai H and Hirai T 2003 Effects of plasticizers on novel electromechanical actuations with different poly(vinyl chloride) gels *J. Polym. Sci. B* **41** 2119–27
- [12] Bae J W, Shin E-J, Jeong J, Choi D-S, Lee J E, Nam B U, Lin L and Kim S-Y 2017 High-performance PVC gel for adaptive micro-lenses with variable focal length *Sci. Rep.* **7** 1–8
- [13] Li Y and Hashimoto M 2015 PVC gel based artificial muscles: characterizations and actuation modular constructions *Sens. Actuators A* **233** 246–58
- [14] Frank Z, Olsen Z, Hwang T and Kim K J 2021 A multi-degree of freedom bending actuator based on a novel cylindrical polyvinyl chloride gel *Proc. SPIE 11587, Electroactive Polymer Actuators and Devices (EAPAD) XXIII* vol 11587 p 17
- [15] Lan C, Zhou Z, Ren H, Park S and Lee S H 2019 Fast-response microlens array fabricated using polyvinyl chloride gel *J. Mol. Liq.* **283** 155–9
- [16] Hirai T, Ogiwara T, Fujii K, Ueki T, Kinoshita K and Takasaki M 2009 Electrically active artificial pupil showing amoeba-like pseudopodial deformation *Adv. Mater.* **21** 2886–8
- [17] Li Y, Guo M and Li Y 2019 Recent advances in plasticized PVC gels for soft actuators and devices: a review *J. Mater. Chem. C* **7** 12991–3009
- [18] Hirai T 2007 Electrically active non-ionic artificial muscle *J. Intell. Mater. Syst. Struct.* **18** 117–22
- [19] Ali M and Hirai T 2012 Effect of plasticizer on the electric-field-induced adhesion of dielectric PVC gels *J. Mater. Sci.* **47** 3777–83
- [20] Ali M and Hirai T 2012 Relationship between electrode polarization and electrical actuation of dielectric PVC gel actuators *Soft Matter* **8** 3694–9
- [21] Asaka K and Hashimoto M 2018 Electrical properties and electromechanical modeling of plasticized PVC gel actuators *Sens. Actuators B* **273** 1246–56
- [22] Ben Ishai P, Talary M S, Caduff A, Levy E and Feldman Y 2013 Electrode polarization in dielectric measurements: a review *Meas. Sci. Technol.* **24** 102001
- [23] Xu P and Zhang X 2011 Investigation of MWS polarization and dc conductivity in polyamide 610 using dielectric relaxation spectroscopy *Eur. Polym. J.* **47** 1031–8
- [24] Hirai T et al 2003 Quick and large electrostrictive deformation of non-ionic soft polymer materials *Proc. SPIE 5051, Smart Structures and Materials 2003: Electroactive Polymer Actuators and Devices (EAPAD)* vol 5051 pp 198–206
- [25] Sato H and Hirai T 2013 Electromechanical and electro-optical functions of plasticized PVC with colossal dielectric constant *Proc. SPIE 8687, Electroactive Polymer Actuators and Devices (EAPAD) 2013* vol 8687 p 868728
- [26] Asaka K and Hashimoto M 2020 Electromechanical modeling of plasticized PVC gel actuators and the improvement in their performances with the additions of ionic liquids *Proc. SPIE 11375, Electroactive Polymer Actuators and Devices (EAPAD) XXII* vol 10594 p 1059408
- [27] Frank Z, Olsen Z, Hwang T and Kim K J 2019 Modelling and experimental study for PVC gel actuators *ASME 2019 Dynamic Systems and Control Conf., DSCC 2019* vol 3 pp 1–9
- [28] Shibagaki M, Ogawa N and Hashimoto M 2010 Modeling of a contraction type PVC gel actuator *2010 IEEE Int. Conf. on Robotics and Biomimetics* pp 1434–9
- [29] Shibagaki M, Hayasaka N and Hashimoto M 2012 Position control of a contraction type PVC gel actuator *Trans. Soc. Instrum. Control Eng.* **48** 45–50
- [30] Karmakar A and Ghosh A 2012 Dielectric permittivity and electric modulus of polyethylene oxide (PEO)-LiClO₄ composite electrolytes *Curr. Appl. Phys.* **12** 539–43
- [31] Tsangaris G M, Psarras G C and Kouloumbi N 1998 Electric modulus and interfacial polarization in composite polymeric systems *J. Mater. Sci.* **33** 2027–37
- [32] Tian F and Ohki Y 2014 Electric modulus powerful tool for analyzing dielectric behavior *IEEE Trans. Dielectr. Electr. Insul.* **21** 929–31
- [33] Hwang T, Frank Z, Neubauer J and Kim K J 2019 High-performance polyvinyl chloride gel artificial muscle actuator with graphene oxide and plasticizer *Sci. Rep.* **9**
- [34] Daniels P H 2009 A brief overview of theories of PVC plasticization and methods used to evaluate PVC-plasticizer interaction *J. Vinyl Addit. Technol.* **21** 219–23
- [35] Sharma P, Kanchan D K, Pant M and Singh K P 2010 Conductivity studies in proton irradiated

- AgI-Ag₂O-V₂O₅-TeO₂ super-ionic glass system *Mater. Sci. Appl.* **01** 59–65
- [36] Pal P and Ghosh A 2020 Broadband dielectric spectroscopy of BMPTFSI ionic liquid doped solid-state polymer electrolytes: coupled ion transport and dielectric relaxation mechanism *J. Appl. Phys.* **128** 084104
- [37] Abdul Halim S I, Chan C H and Apotheker J 2021 Basics of teaching electrochemical impedance spectroscopy of electrolytes for ion-rechargeable batteries—part 2: dielectric response of (non-) polymer electrolytes *Chem. Teach. Int.* **3** 117–29
- [38] Mahmoud W E and Al-Ghamdi A A 2010 The influence of vanadium pentoxide on the structure and dielectric properties of poly(vinyl alcohol) *Polym. Int.* **59** 1282–8
- [39] Ali M, Ueki T, Hirai T, Sato T and Sato T 2013 Dielectric and electromechanical studies of plasticized poly(vinyl chloride) fabricated from plastisol *Polym. Int.* **62** 501–6
- [40] Cole K S and Cole R H 1942 Dispersion and absorption in dielectrics: II. Direct current characteristics *J. Chem. Phys.* **10** 98–105
- [41] Coelho R 1983 Sur la relaxation d'une charge d'espace *Rev. Phys. Appl.* **18** 137–46
- [42] Klein R J, Zhang S, Dou S, Jones B H, Colby R H and Runt J 2006 Modeling electrode polarization in dielectric spectroscopy: ion mobility and mobile ion concentration of single-ion polymer electrolytes *J. Chem. Phys.* **124** 144903
- [43] Kammer H-W 2019 About dielectric relaxation in highly cross-linked poly(ethylene oxide) *Ionics* **25** 2633–43
- [44] Meyer R, Waser R, Prume K, Schmitz T and Tiedke S 2005 Dynamic leakage current compensation in ferroelectric thin-film capacitor structures *Appl. Phys. Lett.* **86** 1–3
- [45] Xia H and Hirai T 2010 Electric-field-induced local layer structure in plasticized PVC actuator *J. Phys. Chem. B* **114** 10756–62
- [46] Yamamoto A, Nakashima T and Higuchi T 2007 Wall climbing mechanisms using electrostatic attraction generated by flexible electrodes *2007 Int. Symp. Micro-NanoMechatronics Hum. Sci. MHS* pp 389–94
- [47] Izadi H and Penlidis A 2013 Polymeric bio-inspired dry adhesives: van der Waals or electrostatic interactions? *Macromol. React. Eng.* **7** 588–608
- [48] Ali M, Ueki T, Tsurumi D and Hirai T 2011 Influence of plasticizer content on the transition of electromechanical behavior of PVC gel actuator *Langmuir* **27** 7902–8